Acta Protozool. (2002) 41: 383 - 396

ACTA
PROTOZOOLOGICA

Development of *Schroedera plumatellae* gen. n., sp. n. (Microsporidia) in *Plumatella fungosa* (Bryozoa: Phylactolaemata)

David J. MORRIS and Alexandra ADAMS

Institute of Aquaculture, University of Stirling, Stirling, Scotland, U.K.

Summary. A new microsporidian, *Schroedera plumatellae*, is described infecting a freshwater bryozoan. The development of the infection is described both at the light and ultrastructural level. The infection induces the formation of hyperplastic testes within the bryozoan host from which cord-like xenomas form. Development of diplokaryotic sporonts is preceded by haplophasic schizogony. Sporogony forms diplokaryotic spores. The spores formed within the xenomas are oval, tapering to one end and were 7.2 ± 0.3 μm by 5.0 ± 0.3 μm with 22-23 turns of the polar filament. Sporogony occurred within the hyaloplasm with the exospore developing into two distinct layers. Phylogenetic analysis showed that the parasite was most closely related to a *Bacillidium* sp. and *Janacekia debaisieuxi*.

Key words: *Bacillidium,* Bryozoa, Microsporidia, *Plumatella fungosa*, *Schroedera plumatellae* gen. n., sp. n.

INTRODUCTION

Phylactolaemate bryozoans are colonial, filter-feeding, hermaphrodites. The testes of these bryozoans develop on the funiculus, a cord of peritoneal cells and muscle fibres that connect the stomach caecum with the body wall. In 1892, Korotneff described a parasite developing within the spermatogonia of *Plumatella fungosa* (Pallas). This parasite was initially named *Myxosporidium bryozoides* within the group "Myxosporidien" but was then transferred into the microsporidian genus *Glugea* (Thélohan 1895). Labbé subsequently transferred the parasite to the genus *Nosema* in 1899.

Since its initial description, *Nosema bryozoides* has been reported in several species of freshwater Bryozoa from around the world. However, these descriptions vary both for the form of the spore and the development of the parasite within the bryozoan hosts. Differences for the site of infection have also been noted between authors. For example, Korotneff (1892) described the development of the parasite as occurring exclusively within the spermatogonia of the bryozoan while Marcus (1941), describing the parasite within *Stolella evelinae* (Marcus), observed parasite development not only within the spermatogonia but also affecting the epithelial cells of the body wall. Marcus (1941) further described the parasite as forming elongated cords from the funiculus that filled the coelom of the bryozoan. These cords are

Address for correspondence: David J. Morris, Institute of Aquaculture, University of Stirling, Stirling FK9 4LA, Scotland, U.K.; Fax: +44 1786 472133; E-mail: djm4@stir.ac.uk

contrary to the lobules figured by Korotneff (1892) and Braem (1911). Schröder (1914) comparing the reports of Korotneff (1892) and Braem (1911), highlighted differences between them regarding the development of the parasite, although he attributed this to different interpretations made on the same parasite species. However, Schröder in his paper also included his own observations on *N. bryozoides* and reported on the development of ellipsoidal spores of two different sizes that slightly tapered to one end. The measurements given for the spores also differ between authors. These differences, particularly between the papers of Schröder (1914) and Marcus (1941), suggest that the reports of *N. bryozoides* in the literature are referring to different microsporidian species in bryozoa rather than observations on the same parasite species. Furthermore, the discovery that bryozoans can act as hosts for several species of Myxozoa has led to the suggestion that the parasite described by Korotneff may have been a myxozoan. As such, the name *N. bryozoides* would be synonymous with a myxozoan and therefore could not be used for a microsporidian (Canning *et al.* 1997).

Recently a new species of microsporidian *Nosema cristatellae* has been reported from the bryozoan *Cristatella mucedo* (Canning *et al*. 1997). This parasite was differentiated from previous descriptions of *N. bryozoides* by both its host and tissue specificity. Here we describe a microsporidian infecting the spermatogonia of *P. fungosa*. Development of this parasite is described both at the light and ultrastructual level. Phylogenetic analysis of the parasites' small subunit (SSU) rDNA sequence and aspects of its development suggest that it is a new species that we propose to call *Schroedera plumatellae* gen. n. *et* sp. n. The terms used for the description of the development of this parasite are derived from the glossary of Sprague and Becnel (1999).

MATERIALS AND METHODS

Collection and identification of colony

A bryozoan colony was obtained, attached to a submerged branch collected from the southern end of Airthrey Loch, University of Stirling, Stirling, Scotland in July 2001. Preliminary examination of the colony using a x10 hand lens suggested that it was a single entity with no evidence of fragmentation. It was removed along with the adherent bark, from the branch using a penknife. Macro-invertebrates were carefully removed under an inverted microscope, using forceps and a pipette. The bark pieces were then glued onto the centre of a 9 cm plastic Petri dish using a cyanacrylate adhesive.

Culture and light microscopy of colony

The colony was cultured following the protocol of Morris *et al.* (2002). Briefly, the Petri dishes were suspended vertically in a 7 l plastic aquarium, containing vigorously aerated, artificial freshwater maintained at 20°C. The colony was fed using cultured *Cryptomonas ovata* (Pringsheim), *Synococcus leopoliensis* (Komárek), *Chilomonas paramecium* (Ehrenberg) and *Colpidium striatum* (Stokes). The colony was removed from the aquarium and examined daily at x40 under an Olympus inverted microscope for any parasite development. As bryozoans grown in the laboratory are transparent it is relatively straightforward to identify parasites within them.

At the termination of the study, statoblast morphology was used to verify the infected bryozoan species. The statoblasts were dissected from the colonies and examined with scanning electron microscopy. Observations made on the colony form of the bryozoan, in conjunction with the SEM examination, were used to identify the bryozoan using the published keys of Mundy and Thorpe (1980) and Ricciardi and Reiswig (1994).

Transmission electron microscopy

Portions of colony, were fixed in Karnovsky's fixative for 4 h and rinsed in cacodylate buffer (pH 7.2) overnight. They were then post-fixed in 1% osmium tetroxide for 1 h, dehydrated through an acetone to alcohol series and embedded in Spurr's resin. Ultrathin gold/silver sections were mounted on formvar coated grids and stained with lead citrate and uranyl acetate. The sections were viewed at 80kV using a Phillips 201 electron microscope. Semi-thin sections (1 μm) were also taken from the blocks, stained with methylene blue-fuchsin for examination of infected tissue using light microscopy.

Molecular characterisation

A portion of colony, consisting of 3 zooids that possessed hyperplastic testes was removed and the DNA extracted using an ABGene Magnetic separation kit following the manufacturers protocol. The small subunit (SSU) rDNA gene from this DNA was amplified using primers V1f and 1942r in a PCR reaction as described by Nilsen (2000). When visualised on a gel, this gave a product of the expected size of ~1300bp. This product was excised from the gel and the DNA purified using a GFX column (Pharmacia). The product was sequenced directly with the original primers and a further two sequencing primers '5-TACCAGGGCCGAATGTTTTA-3' and '5-TCACTACCTCTCCCCATAGGGA-3' using the DYEnamic sequencing kit (Amersham Pharmacia). The sequencing was performed on an ABI Prism 377 sequencer (Perkin Elmer). The initial PCR reaction was repeated and the product sequenced as before to confirm the final sequence.

Phylogenetic analysis

The obtained SSU sequence was aligned to other microsporidial sequences obtained on the GenBank database using ClustalX. These sequences were as follows: *Amblyospora californica* (U68473); *Amblyospora* sp. (U68474); *Amblyospora connecticus* (AF25685); *Amblyospora stimuli* (AF027685); *Bacillidium* sp. (AF104087); *Culicosporella lunata* (AF027683); *Edhazardia aedis* (AF027684);

Encephalitozoon cuniculi (L39107); *Encephalitozoon hellem* (L39108); *Endoreticulatus schubergi* (L07123); *Glugea anomala* (AF104084); *Glugea atherinae* (U15987); *Ichthyosporidium* sp. (L39110); *Janacekia debaisieuxi* (AJ252950); *Kabatana takedai* (AF356222); *Loma* sp. (AF104081); *Microgemma* sp. (AJ252952); *Microsporidium prosopium* (AF151529); *Nosema algerae* (AF069063); *Nosema bombi* (U26158); *Nosema bombycis* (D85504); *Nosema carpocapsae* (AF426104); *Spraguea lophii* (AF0104086); *Thelohania solenopsae* (AF134205); *Trachipleistophora hominis* (AJ002605); *Vairimorpha necatrix* (Y00266); *Vavraia oncoperae* (X74112); *Visvesvaria acridophagus* (AF024658); *Visvesvaria algerae* (AF024656) and *Vittaforma corneae* (L39112). Regions of ambiguous alignment were visually identified and removed. Phylogenetic analyses were conducted on the aligned sequences using MEGA version 2.1 (Kumar *et al.* 2001). The data were analysed using maximum parsimony analysis and neighbour-joining for distance analysis with the Kimura-2 algorithm. Maximum likelihood analysis was also performed on the aligned sequences using fastDNAml (Felsenstein 1981, Olsen *et al*. 1994).

RESULTS

Bryozoa colony

After one week the bryozoan colony, growing on the surface of the Petri dish, appeared parasite free. After 27 days in culture, a portion of the colony appeared to be parasitised. The infection eventually spread throughout the whole colony.

Infected portions of the colony did not produce mature statoblasts, however it was possible to extract mature statoblasts from those branches of the colony that had grown onto the Petri dish before the infection became apparent. Examination of these statoblasts using SEM determined that the bryozoan was *Plumatella fungosa*.

Examination of Microsporidia development by examination of live colonies

The initial observation of parasitised zooids consisted of single cells appearing on the peritoneum of the funiculus of a zooid (Fig. 1). These cells appeared to replicate, forming bundles of cells along the funiculus (Figs 2, 3). As the infection progressed, the cell bundles produced flagella that hung in the coelom of the bryozoan, wafting in currents of coelomic fluid (Fig. 4). The development of the tissue at this point was indistinguishable from that for the spermatogonia of normal phylactolaemate bryozoan testes. However, unlike normal testes, more of the funiculus became replaced with spermatogonia until it appeared to be totally comprised of these cells. The length of the tissue continued to grow until it was up to three times the length of a normal funiculus (Fig. 5). Seven days after the initial spermatogonic cells were noted, the proliferation of cells appeared to halt and a second developmental phase started (Fig. 6). This took the form of the spermatogonic cells becoming hypertrophied, developing into elongate cord-like xenomas, that hung freely in the coelom of the bryozoan. Flagella were not observed on these cords. As more of the infected cells developed into cords, they totally filled the coloemic space entwining together, forming a tangled mass that surrounded the zooid and the coelom immediately posterior to it (Fig. 7). These masses gave the infected zooids an opaque, white appearance when viewed by the naked eye. Within many of the cords microsporidian spores and developmental stages could be observed (Fig. 8). During this time constrictions were noted along the length of some of the cords, eventually leading to bundles of spores being pinched off (Fig. 9). The bundles of spores being delimited by the plasma membrane of the host cell. The cytoplasm surrounding the spore bundles reduced until it appeared as a thin walled sac. When the coelom had become filled with the parasitised cells the zooid possessing the infected funiculus began to atrophy and degenerate. The degeneration of the zooid sealed the coelom containing the spore masses from the rest of the bryozoa colony, forming a sealed tube full of spore bundles. This portion of the colony containing the spore bundles would gradually shrink until only an opaque mass of spores contained within the chitinous remains of the bryozoan remained (Fig. 10).

Development of hyperplastic testes occurred on all of the zooids in the infected colony. Although the parasite apparently induced testes development and spermatogenesis, mature spermatozoa were never observed, suggesting that the bryozoan was effectively castrated by the infection. Development of statoblasts although noted to begin during the early stages of infection (Fig. 2) was suppressed on parasitised zooids and presumably the developing statoblasts were absorbed as the parasite infection progressed along the funiculus. Parasite development was only ever observed associated with the funiculus of the bryozoan. No other tissues apart from those on the funiculus were noted to be infected with the microsporidian.

Some spore bundles that had become detached from the main mass of spores were observed free in the coelom of the bryozoan host moving from the diseased zooid into 'healthy' areas of the colony. These bundles were ejected from the bryozoan by the lophophore of

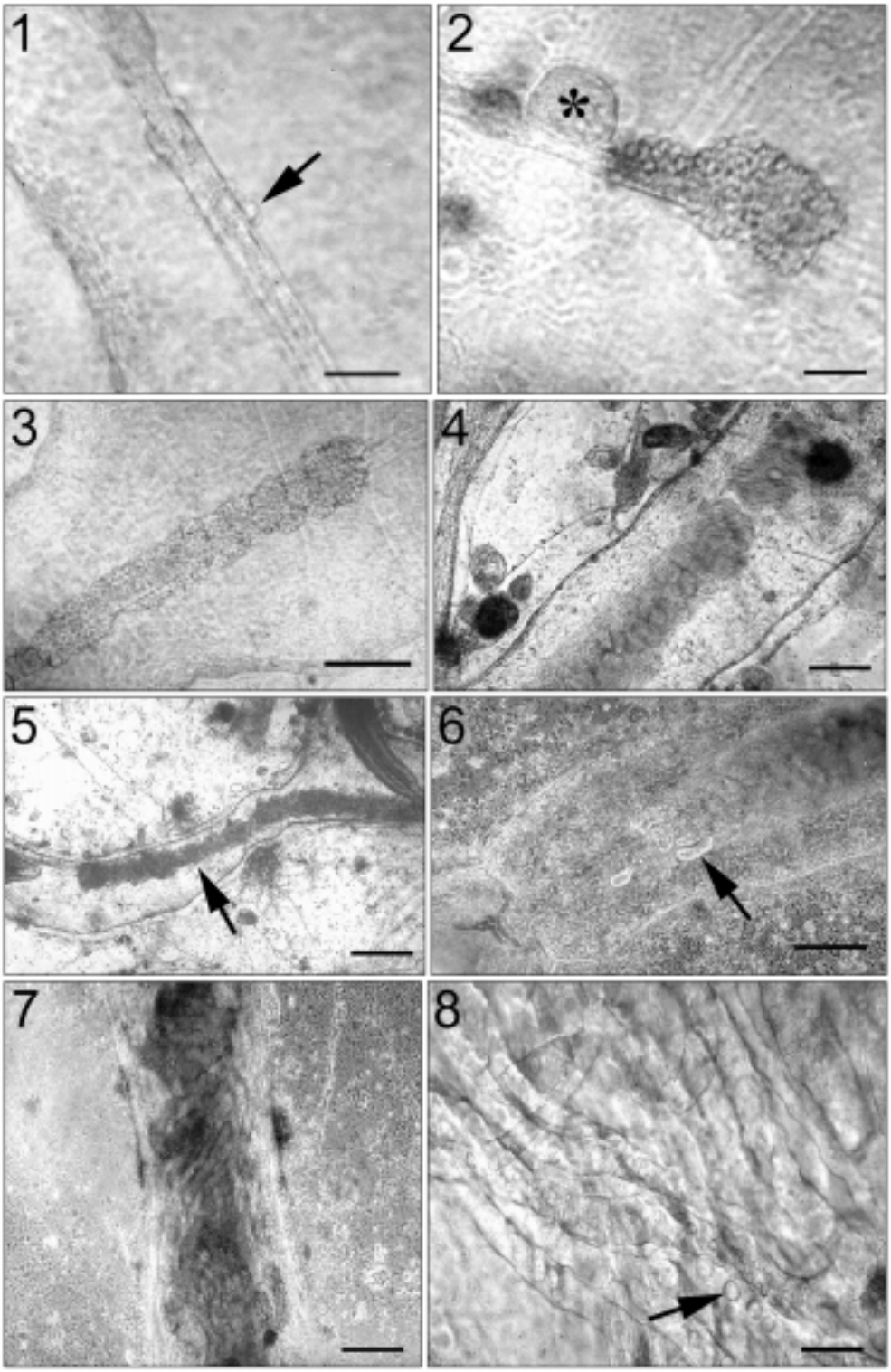

Figs 1 - 8. *Schroedera plumatellae* sp. n. **1** - first sign of infection on the funiculus in a living colony of Bryozoa. Arrow indicates cell developing from the peritoneum of funiculus; **2** - development of clump of cells on funiculus. An immature statoblast is also developing upon the funiculus (*); **3** - continued development of cells along the funiculus; **4** - development of spermatids on funiculus, the infected tissue resembling testis with the tails of the spermatids visible hanging in the coelom of the bryozoan; **5** - hyperplasia of spermatogonic tissue. Arrow indicates the expected length of a non-infected funiculus; **6** - start of development of cord-like xenomas from the infected spermatogonia (arrow); **7** - coelom of bryozoan completely filled with cord-like xenomas derived from the spermatogonia; **8** - detail of cord-like xenomas within bryozoan coelom. Within the xenomas developing microsporidian spores can be observed (arrow). Scale bars: 1, 2 - 20 μm; 3 - 100 μm; 4, 6, 7 - 150 μm; 5 - 350 μm; 8 - 30 μm

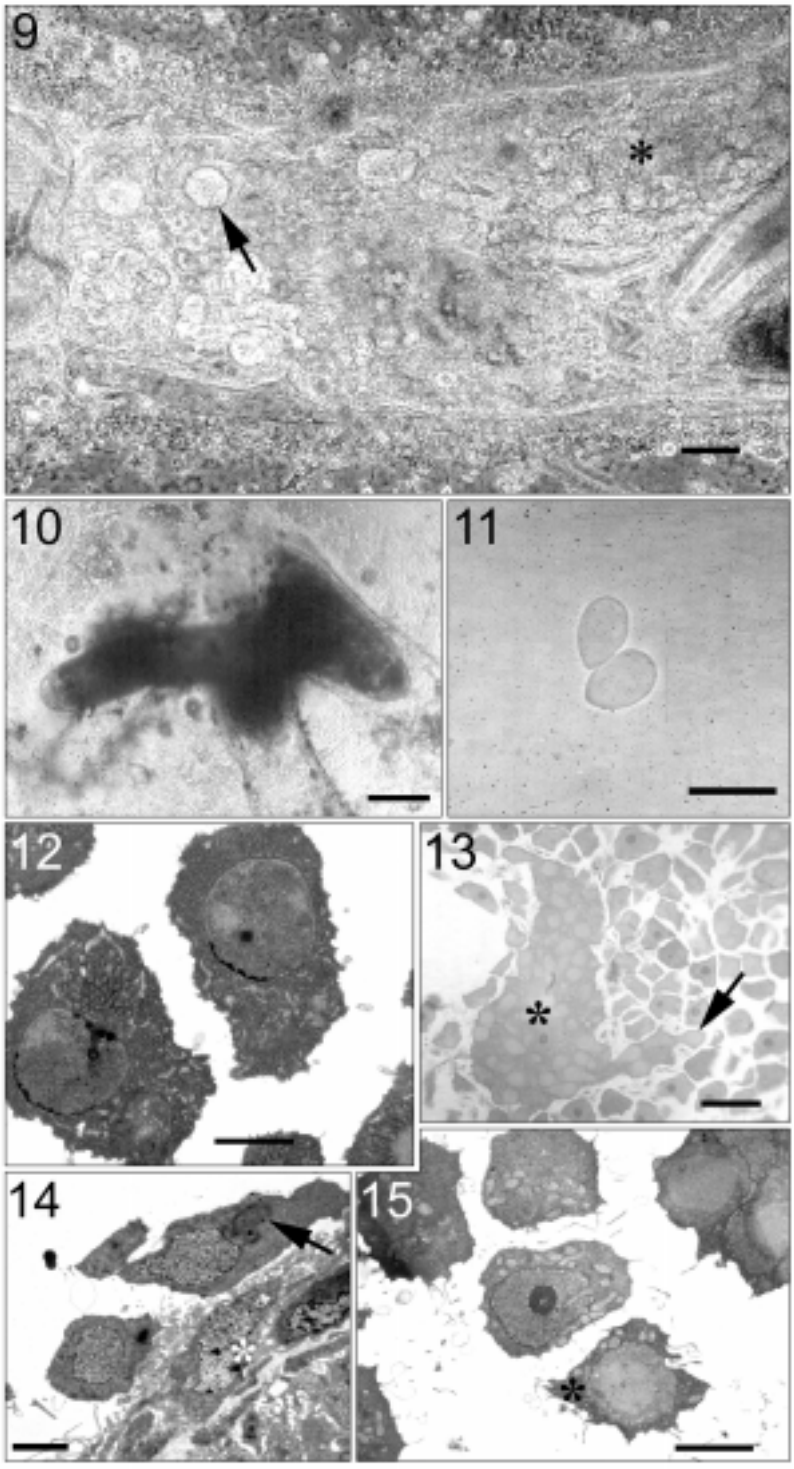

Figs 9-15. *Schroedera plumatellae* sp. n. **9** - breakdown of xenomas into spore bundles. Arrows indicate discrete bundles of spores that have separated from the xenomas. As more spores develop within the cord-like xenomas the cytoplasm reduces giving the cords a knotted appearance (*). Phase contrast microscopy; **10** - dead part of bryozoan colony filled with spore bundles, giving it an opaque appearance; **11** - fresh spores of *S. plumatellae*; **12** - spermatids associated with normal testis development observed in infected bryozoan colony. Heterochromatin is clearly deposited near the nuclear membrane, with mitochondria clustering around the forming midpiece; **13** - spermatogonic cell (*) infected with haplophasic schizonts. This cell is surrounded by numerous associated spermatids. Note the lobed appearance of parts of the spermatogonic cell (arrow); **14** - spermatids, associated with infected spermatogonic cell, adjacent to the peritoneum of the bryozoan coelom (*). Note irregular shaped nuclei of spermatids and presence of an amorphous structure in one of the spermatids (arrow); **15** - spermatids associated with infected spermatogonic cell (top right hand corner). A spermatid (*) is infected with a schizont. Scale bars: 9 - 75 μm; 10 - 350 μm; 11 - 10 μm; 12 - 2 μm; 13 - 20 μm; 14, 15 - 3 μm

both the infected and neighbouring zooids. When this happened the lophophore would retract, and the spore bundle would be released from between the tentacles. The exact route of exit could not be determined due to compression of the tissue during the retraction of the lophophore. Ejected spore bundles were collected by pipette, transferred to a glass microscope slide and placed under a coverslip. Pressure applied on the coverslip allowed the bundle to rupture and for the number of spores within the bundles to be counted under x200 magnification. Using this method, the contents of 6 spore bundles were examined and found to contain variable numbers of spores from 122 to 312. Some spores at this time were noted to partially extrude an isofilar polar filament of over 40 μm in length. Complete extrusion however, was not noted. The spores were ovoid, tapering to one end and measured 5.0 ± 0.3 μm by 7.2 ± 0.3 μm (n=22) (Fig. 11). Very occasionally, larger spores 10.0 μm by 6.0 μm of an identical shape to the smaller spores were observed.

The infection did not affect all of the zooids in a single branch at the same time, although all branches of the colony were finally infected. The development of the parasites appeared to depend upon the age of the zooid. Young and developing zooids at the end of a branch did not appear to be infected. However, the further away from the growing terminal of the branch the zooid was, the more pronounced the infection. This resulted in the colony quickly becoming fragmented for as fast as zooids were produced by the growing end of a branch of the colony, they were dying at the other end of the colony to be replaced by bundles of spores.

Spore sacs naturally extruded from the bryozoans were occasionally observed to be ingested by neighbouring zooids. Although, it could not be determined whether these spores were capable of infecting other zooids or if the subsequent infection of zooids occurred by sharing a common coelom with the infected colony.

Examination of microsporidian development using fixed tissue

Samples for TEM were taken during the infection within the funiculus tissue, during the production of elongate cord-like xenomas and during the degeneration of a zooid.

Infection of the funiculus

Sections through the bryozoan demonstrated areas of normal testis development and other, neighbouring areas that comprised of microsporidian infected spermatogonic cells and affected spermatids. The interface between the infected and non-infected parts of the testis, however, could not be determined.

Normal spermatid development was determined by comparison of these areas of the tissue with a previous ultrastructural description of spermatogenesis for *P. fungosa* (Franzén 1982). The observed spermatids were connected to the funiculus and each other by very fine cytoplasmic filaments. They were characterised by the formation of heterochromatin on the nuclear envelope, insertion of a centriole in the nucleus and the formation of midpiece and tail regions (Fig. 12). Full development of spermatozoa possessing developed acrosomes however was not observed.

In contrast, to the non-infected areas of spermatogonic tissue, the infected areas consisted of hypertrophied spermatogonic cells associated with large numbers of surrounded spermatids. The infected spematogonic cell was irregular in shape with short lobed branches of cytoplasm extending from it (Fig. 13). The spermatids, although connected to each other and the spermatogonic cell with fine cytoplasmic threads appeared to be affected by their association with the infected spermatogonic cell. They possessed irregular shaped nuclei with dispersed heterochromatin, often with a pronounced nucleolus. Centriole and associated midpiece/tail development was not noted although they did contain numerous mitochondria. Some affected spermatids appeared possess areas of amorphous material, possibly resembling degenerating midpieces. A few affected spermatids were observed in direct contact with the peritoneum of the bryozoans' coelom (Fig. 14).

Haplophasic schizonts were noted within the hypertrophic spermatogonic cells of the funiculus, and sometimes in the associated spermatids (Fig. 15). The schizonts possessed a round nucleus that occupied approximately half of the parasites' volume, endoplasmic reticulum and dense bodies (Fig. 16). The schizonts resided in direct contact with the host cells' cytoplasm and appeared to replicate by binary division as no chain or rosette formation was observed. Actual division was not noted. The staining intensity of both the host cells and the schizonts varied, even within the same section, with some schizonts easily distinguished from the host cell while others were not (Fig. 17). This may have been an artefact caused by the staining procedure or variations in section thickness, however as the variations appeared consistent in serial sections and within the same section it may represent developmental differences in the formation of xenomas.

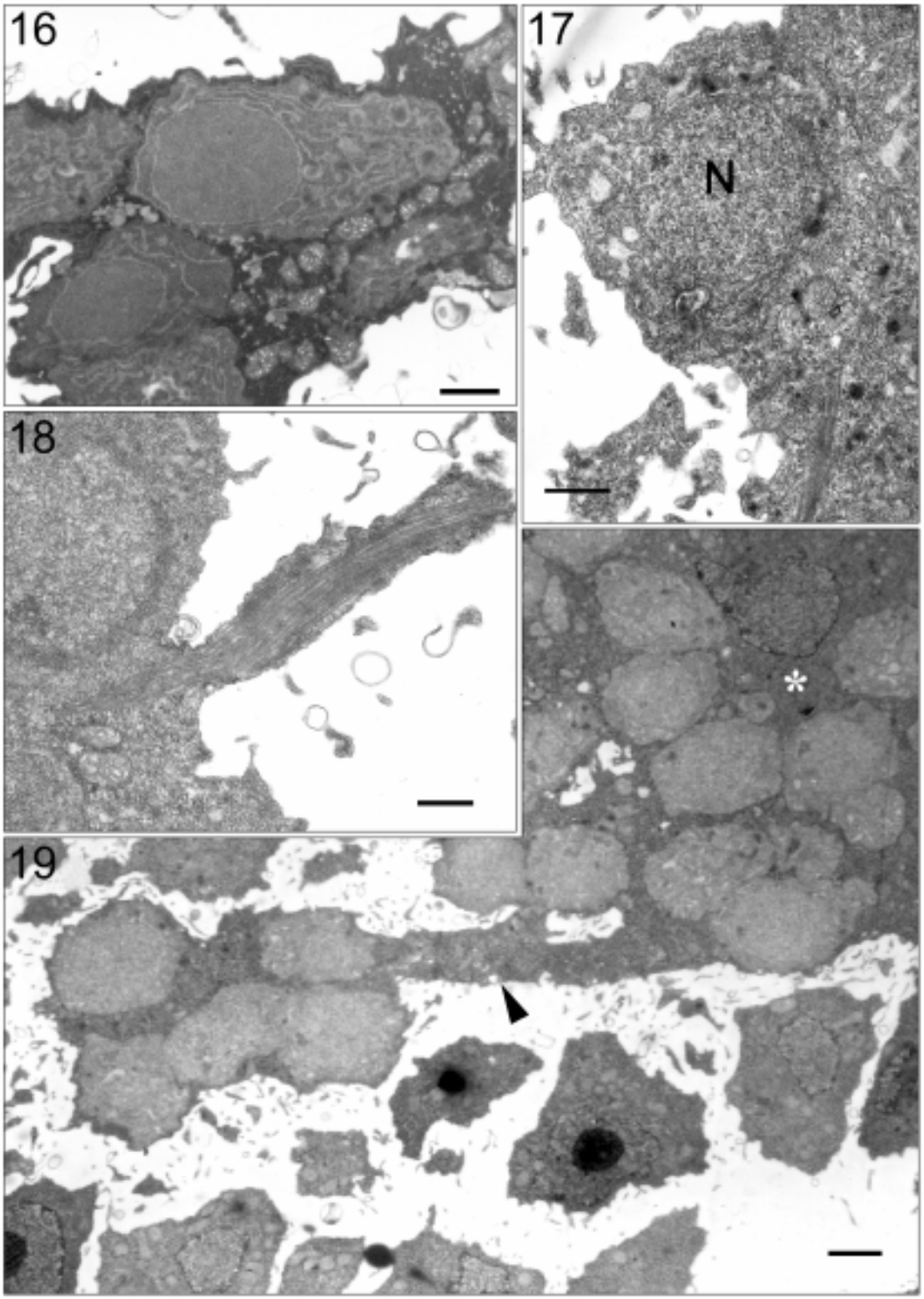

Figs 16-19. *Schroedera plumatellae* sp. n. **19** - haplophasic schizont present in spermatogonic cell. Details of schizont structure clearly visible; **17** - schizont present in spermatogonic cell, poorly differentiated from the host cell cytoplasm. Nucleus of schizont indicated with an N.; **18** - microtubules extending from infected spermatogonic cell; **19** - connection of spermatogonia (*) to schizont infected spermatid *via* cytoplasmic extension of spermatogonia (arrowhead). Scale bars: 16 - 1 μm; 17, 18 - 500 nm; 19 - 2.5 μm

In addition to the spermatogonic cells becoming hypertrophied, bundles of microfilaments were observed extending from the infected spermatogonic cells connecting them to spermatids (Fig. 18). The spermatids connected in this way were always noted to contain one or more schizonts (Fig. 19). Often the microtubules would just be surrounded by a thin layer of cytoplasm, but more substantial connections between spermatids and the spermatogonia existed with mitochondria and other organelles occurring along the length of the connecting microtubules. It could not be ascertained whether the microtubules originated from reorganisation of the spermatogonic cell or the connected spermatid.

Development of xenomas into cords

In section, the cord-like xenomas appeared as discrete hypertrophied cells filling the coelom. Unlike the previous phase of development there were no cells, spermatids or otherwise, associated with the xenomas. The surface of the xenomas possessed many fine cytoplasmic filaments of host cell origin. Microtubular extensions were not noted. The cytoplasm of the xenoma was granular with mitochondria dispersed throughout. The xenomas were multi-nucleated possessing enlarged nuclei, with reduced chromatin. The xenomas possessed many diplokaryotic sporonts within them (Fig. 20). Occasional parasite cells were also observed that appeared haplophasic although this may have been due to the plane of section through a sporont. The nuclei of the sporonts appeared to be of similar size, while the cytoplasm contained rough endoplasmic reticulum. Karyogamy by the haplophasic schizonts to form sporonts, or division of the sporonts however, was not observed. Sporonts were observed developing into sporoblasts. At this stage of development the cytoplasm of the sporont would become indistinct making any nuclear or cellular division difficult to assess (Fig. 21). The membrane of the parasite would become locally electron dense caused by the parasite extending fine membranous processes over its surface. Beneath these processes, material would form that separated the parasite from the host cell (Fig. 22). The membranes and the material between them appeared to condense to form the electron dense surface of the developing sporoblast. Complete separation of the parasite and the cytoplasm of the host cell by the formation of an interfacial envelope was not observed.

Early development of sporoblasts was observed within the cords. These stages were oval, and had an electron dense thickening of their plasmalemma, the cytoplasm appearing to be relatively electron lucent compared to that of sporonts and schizonts (Fig. 23). Fixation of the developing sporoblasts was poor and so the processes of sporogony could not be determined.

Spore morphology

Examination of the spore mass collected from a degenerating zooid determined that the host cell cytoplasm was very reduced, composed of occasional mitochondria in an electron lucent granular material with spores, sporoblasts and occasional sporonts. Haplophasic schizonts were not present at this stage of the infection.

Fixation of the majority of spores was poor. Mature spores were observed to lie directly within the host cell cytoplasm. The fixed spores appeared to be oval, tapering to one end. The spores observed all appeared to be of one type, larger spores as noted under light microscopy were not observed in the sections examined. The spore wall consisted of an electron lucent endospore surrounded by an exospore of two distinct layers. An electron dense layer, surrounded by a glycocalyx-like, granular layer, that could be easily distinguished from the cytoplasm of the host cell (Fig. 24). The thickness of the two outer layers was roughly equal, measuring between 200-250 nm thick except anteriorly, where it was down to 150 nm thick. The electron-dense exospore layer of some spores was observed to possess fine ornamentation towards the anterior and posterior poles, reminiscent of small bubbles (Fig. 25). The spores were diplokaryotic, with nuclei of roughly equal size arranged in tandem. Encircling the nuclei were well-developed cisternae of rough endoplasmic reticulum. The polar filament appeared to be isofilar and was coiled 22-23 times in one to three rows around the spore (Fig. 26). An electron dense body of unknown function was observed at the base of the polaroplast in one of the spores. The polar filament was composed of three layers, alternating between electron lucent and electron dense, with an electron dense core (Fig. 27). The polaroplast consisted of closely packed anterior lamellae with wider less organised posterior lamellae, with a surrounding electron-dense, bell shaped polar sac. The posterior vacuole of the spore contained granular material (Fig. 28).

rDNA analysis

A segment of the SSU rDNA of the parasite was successfully amplified by PCR and sequenced. This segment was 1348 bp in length with a GC content of 42.7%. The Genbank/NCBI accession number is AY135024. When using the BLAST facility, the se-

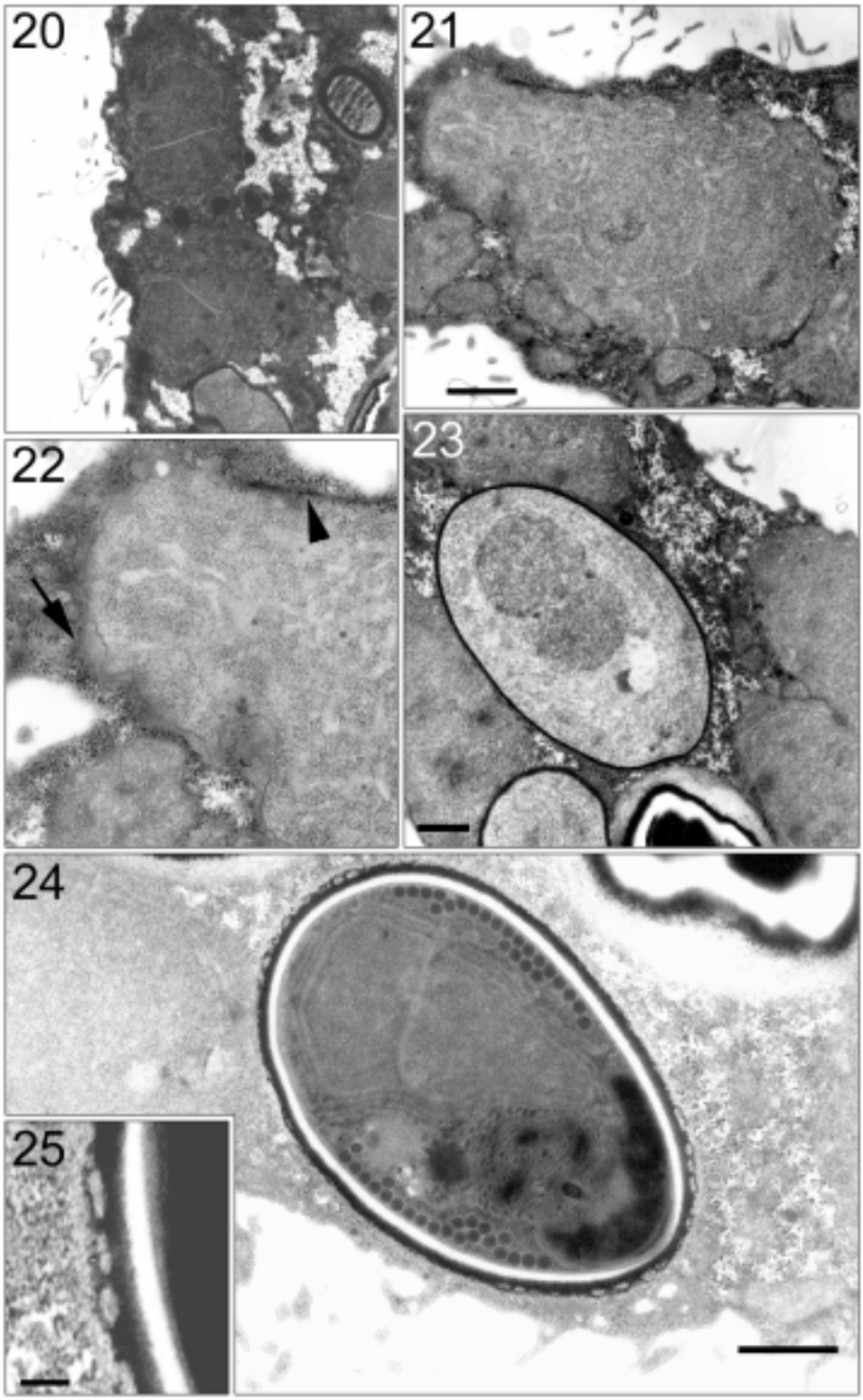

Figs 20-25. *Schroedera plumatellae* sp. n. **20** - diplokaryotic sporonts. **21** - transformation of sporont into sporoblast. Cytoplasm of the cell becomes increasingly lucent making differentiation of the nuclei difficult; **22** - detail of Fig. 21 demonstrating formation of electron-dense cell membrane of sporoblast. Arrow indicates membranous extensions derived from sporont. Arrow-head indicates condensing of material to form electron-dense membrane; **23** - Sporoblast with electron-dense cell membrane; **24** - spore, demonstrating bubble-like formations on the exospore; **25** - detail of Fig. 24 showing bubble-like extensions to the electron-dense layer of the exospore. Scale bars: 20 - 2 μm; 21 - 1 μm; 22 - 500 nm; 23 - 1 μm; 24 - 1 μm; 25 - 200 nm

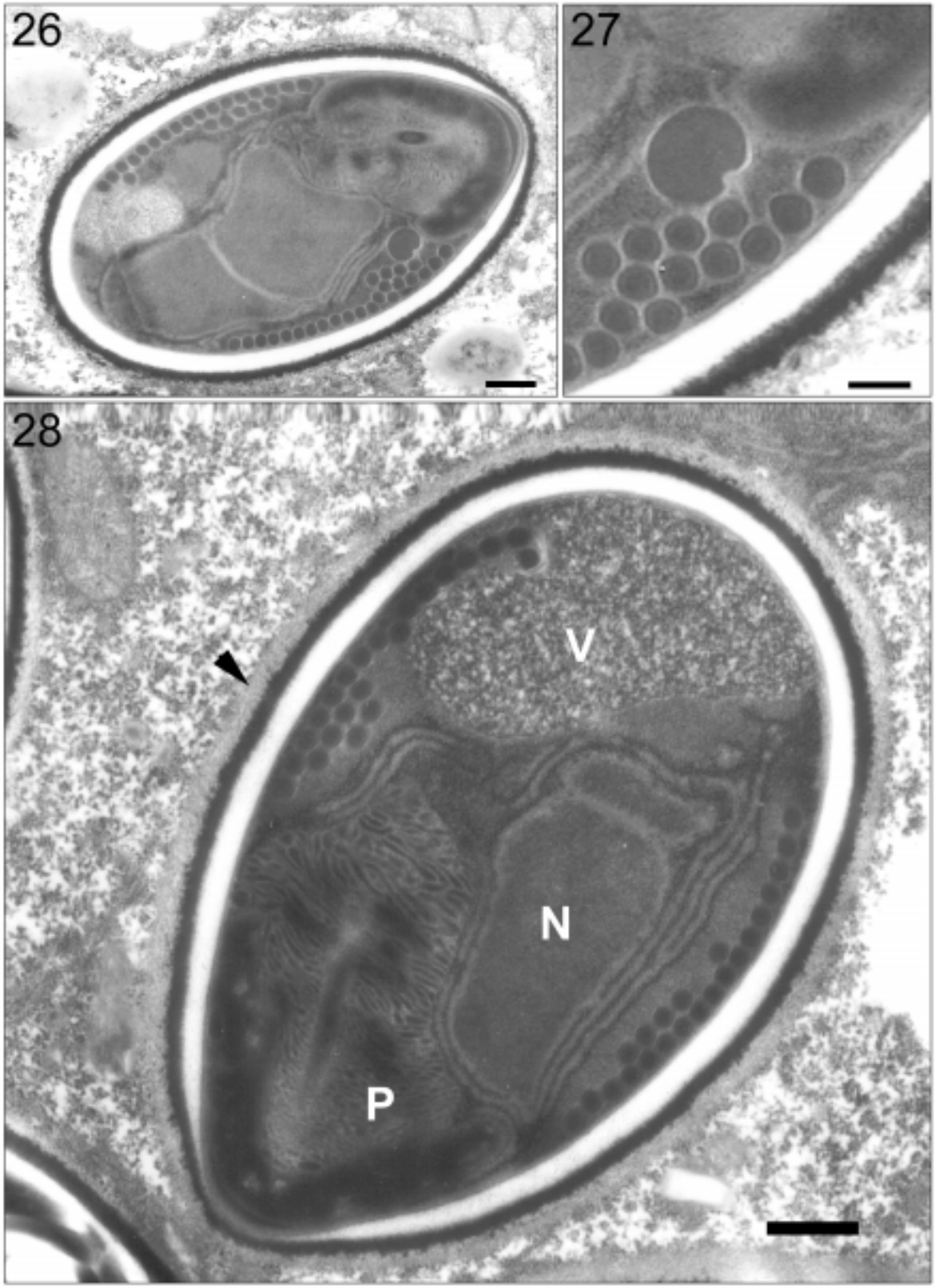

Figs 26-28. 26 - *Schroedera plumatellae* sp. n. spore with nuclei of similar sizes and location of unidentified body at the base of the polaroplast; **27** - detail of Fig. 26 highlighting the unidentified body and the structure of the polar filament; **28** - spore of demonstrating granular posterior vacuole (V), lamellae nature of the polaroplast (P), diplokaryon (N) and two distinct layers of material forming the exospore (arrowhead). Scale bars: 26 - 500 nm; 27 - 200 nm; 28 - 500 nm

quence showed highest homology to the sequence in Genbank deposited for *Bacillidium* sp. (AF104087) and *Janacekia debaisieuxi* (AJ252950). Using parsimony, distance analysis and maximum likelihood analysis, trees with very similar overall topology were obtained. All of the analyses consistently placed *S. plumatellae* in a group branching with *Bacillidium* sp. and *J. debaisieuxi* (Fig. 29). The bootstrap support for this group was 100%, independent of the method used. This group appeared within a larger clade that included *Nosema algerae, Thelohania solenopsae, Visvesvaria algerae* and *V. acridophagus*. The grouping of *N. algerae* with *V. algerae* is in accordance to the previous phylogenetic studies on this species that distanced it from other *Nosema* spp. (Müller *et al*. 2000).

DISCUSSION

Only two species of Microsporidia have been identified as parasites of phylactolaemate bryozoans, *Nosema cristatellae* and *N. bryozoides*. The parasite described in this paper is different to the description of *N. cristatellae* in that the host species, host cell type and morphology of the spore are different and therefore we consider that it is not the same species as the parasite described here.

The descriptions of *N. bryozoides* by Korotneff (1892) and Braem (1911) and that of *S. plumatellae* in this study are similar, in that the parasites affect the spermatogonia, are released into the coelom and finally kill the host zooid resulting in a spore filled tube. However, significant differences also exist, *N. bryozoides* is figured to form lobules that develop on the funiculus before detaching to float in the coelom, gradually filling it. The cord-like xenomas observed for *S. plumatellae* were not reported. Marcus (1941) described cord-like xenomas in his description of *N. bryozoides*, however, this author also observed somatic cells becoming infected. These cells were never noted to become infected either in the study presented here or in the previous reports for *N. bryozoides*. As such, it is likely that the parasites described by previous authors are not *S. plumatellae* but other, perhaps related, microsporidian species.

Nilsen (1999) examined the molecular phylogeny of a *Bacillidium* sp. and could not relate it to any other microsporian species included in his analysis. The analysis also demonstrated the presence of four lineages within the Microsporea. The phylogenetic analysis in the present study again suggested four distinct lineages. The *Bacillidium* sp. grouping with *S. plumatellae* and *Janacekia debaisieuxi* which branch from a sister group composed of *Visvesvaria acridophagus, Thelohania solenopsae and Visvesvaria algerae.* The spores of both *Bacillidium* sp. and *J. debaisieuxi* are distinctly different to that of *S. plumatellae*. Members of the genus *Bacillidium* are characterised by rod-shaped spores with a manubroid polar filament, while *J. debaisieuxi* forms oval, uninucleate spores and produces sporogonial plasmodia. Due to these differences it is surprising to find that *J. debaisieuxi* and the *Bacillidium* sp. cluster together in the analyses. The relationship between these species should be examined in more detail as it is possible that they have a life-cycle that involves different forms of spore pertaining to different hosts. Although it has to be noted that the taxonomy of *J. debaisieuxi* is in doubt as it has been suggested that it comprises an assemblage of different species (Sprague *et al.* 1992).

Although *S. plumatellae* does not appear to share many features with *J. debaisieuxi* it does have some common features with the genus *Bacillidium* and other members of the family Mrazekiidae. Notably that sporulation occurs within the host cell hyaloplasm, it is disporous with diplokaryotic nuclei lying in tandem within the spore and it forms a distinctive xenoma. The structure of this xenoma includes fine cytoplasmic extensions on the xenomas' surface and multiple nuclei correlating to the those formed by *Bacillidium criodrili* and *Hrabyeia xerkophora* (Larsson 1986, Lom and Dyková 1990). Furthermore, the differentiation of the exospore into different layers is in keeping with other members the family Mrazekiidae. Usually members of the family Mrazekiidae have rod-like spores, however the genus *Hrabyeia*, is the notable exception to this, forming a tail from the electron-dense exospore material of an ovoid spore. This exospore material being surrounded by a glycocalyx-like layer (Lom and Dyková 1990). We consider that the developmental and phylogenetic data collected during the study of *S. plumatellae* suggest that it is a member of the Mrazekiidae. Although similar to *H. xerkophora* regarding aspects of the spore wall composition and xenoma formation, the absence of a exospore tail and difference in polaroplast construction, suggest significant differences between these species.

From the results of the light and electron microscopy a developmental pathway for the xenoma can be suggested. The parasite infects spermatogonia inducing spermatogenesis and causing this tissue to become

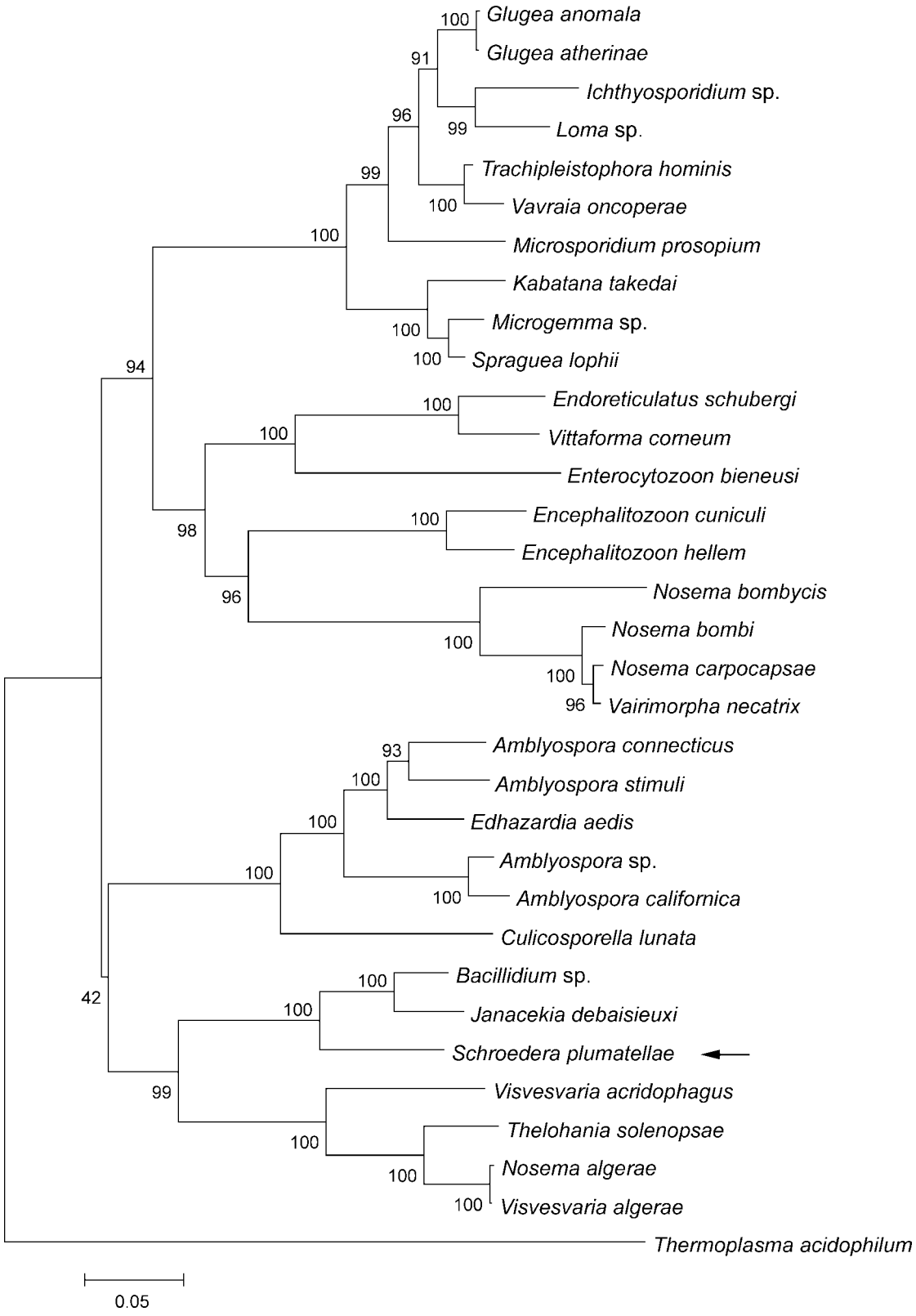

Fig. 29. Tree obtained by 500 bootstrap replicates using Kimura 2-parameter and neighbour joining. The numbers on the branches are a percentage support from the 500 bootstrap resamples. Tree rooted using *Thermoplasma acidophilum* as the outgroup. Branch lengths are proportional to unambiguous changes

hyperplastic. The development of the spermatids associated with the infected spermatogonia into spermatozoa is halted and their development modified, presumably to supply energy and nutrients to the parasitised cell. Either the infected spermatogonia or the connected spermatid develop microtubules that passes to the other cell. This connection allows the cytoplasm of the spermatids and the spermatogonia to fuse, thus forming a multi-nucleated syncitium. Evidence of the fusion of cells is suggested by the lobed appearance of the infected spermatogonia (Figs 13, 19). The microtubules presumably becoming reabsorbed as the two cells merge. As more spermatids are incorporated into the syncitial xenoma so it elongates forming a cord-like structure, with the eventual incorporation of all of the spermatids.

The description of the development of *S. plumatellae* within the host is incomplete. The route of entry into the host is undetermined as are those stages proceeding development on the funiculus. Although it is clear that autoinfection was occurring within the host autoinfective spores were not identified. It is possible that the life cycle of this parasite requires more than one host, and that the microsporidian within this host has already been described. However, until molecular or life-cycle work can elucidate the identity of another host (if there is one) we propose to name the parasite *Schroedera plumatellae* gen. n. *et* sp. n.

TAXONOMY

Schroedera gen. n.

Diagnosis: sporogony diplokaryotic, preceded by haplophasic schizogony. Presumably disporoblastic. Spores are oval, tapering to one end, have an isofilar polar filament arranged in 1-3 rows. The exospore is divided into two distinct layers, an electron dense layer surrounded by a granular layer. Sporophorous vesicles are not produced. The parasite induces xenoma formation that develops in the coelom of the host. Xenomas are multinucleate, derived from interconnected host cells.

Etymology: named in recognition of Dr. Olaw Schröder, who conducted several early studies into bryozoan parasites.

Schroedera plumatellae sp. n.

Schizogony: uninucleate schizonts, divide apparently by binary fission. Number of cycles of schizogony unknown.

Sporogony: presumably disporoblastic. Sporonts diplokaryotic, and develop electron dense surface as they form sporoblasts. Later stages of sporogony did not fix well. Sporophorous vesicle absent.

Spores: ovoid, tapering to anterior end. Dimensions of fresh spores 7.2 x 5.0 μm (±0.3 μm, n=22). A few macrospores observed 10.0 x 6.0 μm. Spore wall as for genus, the two layers forming an exospore 200-250 μm thick. Polar filament, isofilar, composed of three layers of material enclosing an electron dense core, with 22-23 coils arranged in 1-3 rows. The filament is arranged in a single row at the posterior of the spore with 2-3 rows appearing near the anterior of the spore. Thickness of filament 140 nm. Polaroplast with compact membrane vesicles toward anterior and lamellae posteriorly with a surrounding bell shaped, electron dense, polar sac. Polaroplast extends mid-way into the spore. Posterior vacuole contains granular material.

Type host: *Plumatella fungosa* Pallas (Bryozoa, Phylactolaemata)

Host tissue involved: infects spermatogonia to form conspicuous acapsulate xenoma. Host spermatids associated with early xenoma formation.

Type locality: southern end of Airthrey Loch, University of Stirling campus, Stirling, Scotland. The national grid reference being NS 804963.

Type specimens: hapantotype material has been deposited in the collection of the Natural History Museum, London. The material comprises of slides and EM grids of the early stages of parasite development demonstrating schizonts (registration numbers 2002:6:26:1 and 2002:6:26:3) and late stages of development demonstrating sporonts and spore stages (registration numbers 2002:6:26:2 and 2002:6:26:4).

Etymology: name alludes to the host genus.

Acknowledgments. The authors would like to thank Dr. James Bron for advice on sequencing, Dr. Andy Shinn for reviewing the manuscript before submission and Mr. Linton Brown for assistance with the electron microscopy. The authors would also like to acknowledge the Department of Environment, Food and Rural Affairs for funding this research.

REFERENCES

Braem F. (1911) Beiträge zur Kenntnis der Fauna Turkestans. VII. Bryozoen und deren Parasiten. *Trav. Soc. Imp. Nat. St Petersbg.* **42:** 1-56

Canning E., Okamura B., Curry A. (1997) A new microsporidium, *Nosema cristatellae* n. sp. in the bryozoan *Cristatella mucedo* (Bryozoa, Phylactolaemata*). J. Invertebr. Pathol*. **70:** 177-183

Felsenstein J. (1981) Evolutionary trees from DNA sequences: A maximum likelihood approach. *J. Mol. Evol.* **17:** 368-376

Franzén A. (1982) Ultrastructure of spermatids and spermatozoa in the fresh water bryozoan *Plumatella* (Bryozoa, Phylactolaemata). *J. Submicrosc. Cytol*. **14:** 323-336

Korotneff A. (1892) *Myxosporidium bryozoides*. *Z. Wissenschaft Zool*. **53:** 591-596

Kumar S., Tamura K., Jakobsen I. B., Nei M. (2001) MEGA2: Molecular Evolutionary Genetics Analysis software, Arizona State University, Tempe, Arizona, USA

Labbé A. (1899) Sporozoa. In 'Das Tierreich' (Ed. O. Bütschli), Friedländer, Berlin, **5:** 180

Larsson J. I. R. (1986) On the taxonomy of Mrazekidae: resurrection of the genus *Bacillidium* Janda, 1928. *J. Protozool.* **33:** 542-546

Lom J., Dyková I. (1990) *Hrabyeia xerkophora* n. gen. n. sp. a new microsporidian with tailed spores from the oligochaete *Nais cristinae* Kasparzak 1973. *Europ. J. Protist.* **25:** 243-248

Marcus E. (1941) Sôbre bryozoa do Brasil. *Zoologia Univ. Sao Paulo Brazil*. **10:** 3-207

Morris D. J., Morris D. C., Adams A. (2002) Development and release of a malacosporean (Myxozoa) from *Plumatella repens* (Bryozoa: Phylactolaemata). *Folia Parasit. (Praha)* **49:** 25-34

Müller A., Trammer T., Chioralia G., Seitz H. M., Diehl V., Franzen C. (2000) Ribosomal RNA of *Nosema algaerae* and phylogenetic relationship to other microsporidia. *Parasitol. Res.* **86:** 18-23

Mundy S. P., Thorpe J. P. (1980) Biochemical genetics and taxonomy in *Plumatella coralloides* and *P. fungosa* and a key to the British and European Plumatellidae (Bryozoa: Phylactolaemata). *Freshwater Biol*. **10:** 519-526

Nilsen F. (1999) Small subunit rDNA phylogeny of *Bacillidium* sp. (Microspora, Mrazekiidae) infecting oligochaetes. *Parasitology*. **118:** 553-558

Nilsen F. (2000) Small subunit ribosomal DNA phylogeny of Microsporidia with particular reference to genera that infect fish. *J. Parasitol*. **86:** 128-133

Olsen G. J., Matsuda H., Hagstrom R., Overbeek R. (1994) FastDNAml: A tool for construction of phylogenetic trees of DNA sequences using maximum likelihood. *Comput. Appl. Biosci.* **10:** 41-48

Ricciardi A., Reiswig H. M. (1994) Taxonomy, distribution and ecology of the freshwater bryozoans (Ectoprocta) of eastern Canada. *Can. J. Zool*. **72:** 339-359

Schröder O. (1914) Beiträge zur Kenntis einiger Microsporidian. *Zool. Anz*. **43:** 320-327

Sprague V., Becnel J. J. (1999) Glossary. In: The Microsporidia and Microsporidiosis, (Ed. M. Wittner). American Society for Microbiology, Washington D.C., 531-538

Sprague V., Becnel J. J., Hazard E. I. (1992) Taxonomy of Phylum Microspora. *Crit. Rev. Microbiol.* **18:** 285-395

Thélohan P. (1895) Recherches sur les Myxosporidies. *Bull. Sci. Fr. Belg*. **26:** 100-394

Received on 26th March, 2002; accepted on 18th July, 2002